Low-lying isovector 2^{+} valence-shell excitations of ^{212}Po

D. Kocheva *et al.*

Phys. Rev. C **93**, 011303 — Published 19 January 2016

DOI: 10.1103/PhysRevC.93.011303

Low-lying isovector 2^+ valence-shell excitation of ^{212}Po

D. Kocheva,[1] G. Rainovski,[1,*] J. Jolie,[2] N. Pietralla,[3] C. Stahl,[3] P. Petkov,[4,5] A. Blazhev,[2] A. Hennig,[2] A. Astier,[6] Th. Braunroth,[2] M.L. Cortés,[3] A. Dewald,[2] M. Djongolov,[1] C. Fransen,[2] K. Gladnishki,[1] V. Karayonchev,[2] J. Litzinger,[2] C. Müller-Gatermann,[2] M. Scheck,[3,†] Ph. Scholz,[2] R. Stegmann,[3] P. Thöle,[2] V. Werner,[3] W. Witt,[3] D. Wölk,[2] and P. Van Isacker[7]

[1] *Faculty of Physics, St. Kliment Ohridski University of Sofia, 1164 Sofia, Bulgaria*
[2] *Institut für Kernphysik, Universität zu Köln, 50937 Köln, Germany*
[3] *Institut für Kernphysik, Technische Universität Darmstadt, 64289 Darmstadt, Germany*
[4] *Bulgarian Academy of Sciences, Institute for Nuclear Research and Nuclear Energy, 1784 Sofia, Bulgaria*
[5] *National Institute for Physics and Nuclear Engineering,77125 Bucharest-Magurele, Romania*
[6] *CSNSM, IN2P3/CNRS and Universite Paris-Sud, F-91405 Orsay Campus, France*
[7] *Grand Accélérateur National d'Ions Lourds, CEA/DSM-CNRS/IN2P3, BP 55027, F-14076 Caen Cedex 5, France*

We present the results from an experiment dedicated to search for quadrupole-collective isovector valence-shell excitations, states with so-called mixed proton-neutron symmetry (MSS), of ^{212}Po. This nucleus was studied in an α-transfer reaction. The lifetimes of two short-lived excited states, candidates for the one-phonon MSS, were determined by utilizing the Doppler shift attenuation method. The experimental results are in qualitative agreement with a simple single-j shell model calculation, which, together with the observed lack of quadrupole collectivity, indicates that the isovector nature of low-lying states is a property of the leading single-particle valence shell configuration.

PACS numbers: 21.10.Tg, 23.20.Lv, 25.45.Hi, 27.80.+w

States with mixed proton-neutron symmetry (MSSs) are the lowest-lying isovector excitations in the valence shell [1] for vibrational nuclei. Even though these states are defined in the framework of an algebraic model (IBM-2) [2, 3], their properties simultaneously depend on the nuclear quadrupole collectivity, the underlying shell structure, and the proton-neutron balance in the wave function. Mixed-symmetry states are identified experimentally [4, 5] by their strong isovector $M1$ decay to the low-lying fully-symmetric states (FSSs). The best examples of MSSs of stable nuclei are found in the mass A $\approx$ 90 region [4]. In the last decade a large number of MSSs has been identified in the mass A $\approx$ 130 region [6–11].

Although experimental data for MSSs are relatively abundant, especially for properties of one-phonon $2^+_{1,ms}$ states, there are only a few attempts to understand the mechanism that governs the formation and the evolution of these states with the number of nucleons. Heyde and Sau [12] have suggested a schematic model for the formation of isovector excitations in the valence shell which, however, accounts only for the single-particle degree of freedom. Recently, new experimental evidence for the formation mechanism of symmetric and mixed-symmetry low-lying quadrupole collective structures was reported for the $A \approx 90$ region [13]. It has been shown that the one-phonon FS and MS states result from the coupling of the lowest 2-quasiparticle proton and neutron excitations to the Giant Quadrupole Resonance (GQR). Consequently, the $E2$ strengths of these states are dominated by the GQR contributions while the $M1$ properties are determined by the leading valence shell configurations. Within this concept, the strongest $M1$ transitions between one-phonon MSSs and FSSs in a given mass region occur in less collective-vibrational nuclei. These nuclei are, usually, only 2 proton particles (holes) and 2 neutron particles (holes) away from double magic nuclei. Apparently, they will also have the simplest possible valence shell configurations. However, it has also been shown that the absolute $B(M1; 2^+_{1;ms} \rightarrow 2^+_1)$ strength is highly sensitive to the proton-neutron balance of the wave functions; a mechanism dubbed Configurational Isospin Polarization (CIP) [14] occurs when proton and neutron amplitudes in the wave functions of one-phonon 2^+ states are not balanced, and either one dominates. The case of significant CIP is manifested by small absolute $M1$ rates and has first been observed in ^{92}Zr [15]. The opposite case of vanishing CIP leads to a very strong $M1$ transition between the one-phonon MS and FSSs. The combined effect of low collectivity and vanishing CIP has been observed in ^{132}Te [10] - a nucleus which is two protons and two neutron holes away from the doubly magic nucleus ^{132}Sn. It has been shown that the one-phonon MSS of this nucleus, namely the 2^+_2 state, decays with an exceptionally strong $M1$ transition to the FS 2^+_1 state [10]. The opposite case of well pronounced CIP is expected for ^{136}Te [16], due to the expectation that the p-n exchange symmetry is strongly broken as Te and Xe isotopes depart from doubly magic ^{132}Sn [17]. Obviously, to understand better the interplay between collectivity and the isospin degrees of freedom in forming the low-lying isovector excitations, more cases of one-phonon MSSs in the vicinity of double-magic nuclei have to be identified and quantitatively studied. However, nuclei in the

* Corresponding author: (G. Rainovski) rig@phys.uni-sofia.bg
† Present address: University of the West of Scotland, PA1 2BE Paisley, UK and SUPA, Glasgow G12 8QQ, UK

vicinities of double-magic shell closures in which the one-phonon $2^+_{1,ms}$ can be studied experimentally by conventional methods are scarce. In the mass $A \approx 130$ region, *i.e.* the mass region around the double-magic nucleus ^{132}Sn, all such nuclei are neutron-rich and radioactive, including ^{132}Te. The situation around the double-magic nucleus ^{208}Pb is somewhat different. ^{212}Po, which has 2 protons and 2 neutrons more than ^{208}Pb, is experimentally accessible in α-transfer reactions [18]. In this paper the results from such an experiment that proves the existence of a low-lying 2^+ isovector state of ^{212}Po are presented.

The experiment was performed at the FN Tandem facility of the University of Cologne. Excited states of ^{212}Po were populated using the transfer reaction ^{208}Pb(^{12}C,^{8}Be)^{212}Po at a beam energy of 62 MeV. The beam energy was chosen to be about 2 MeV below the Coulomb barrier. The target was a self-supporting 10 mg/cm^2 thick Pb foil enriched to 99.14 % with the isotope ^{208}Pb. The reaction took place in the reaction chamber of the Cologne plunger device [19], in which an array of solar cells was mounted at backward angles with respect to the beam direction, in order to detect the recoiling light reaction fragments. The solar cell array consisted of six 10 mm $\times$ 10 mm cells placed at a distance of about 15 mm between their centers and the target. The array covered an annular space between 116.8° and 167.2°. The γ-rays from the decay of the excited states of ^{212}Po were registered by 12 HPGe detectors mounted outside the plunger chamber in three rings at an average distance of 12 cm from the target. Five detectors were positioned at 142.3° with respect to the beam direction, another six formed a ring at 35° and a single detector was placed at 0°. Data were taken in coincidence mode of at least one solar cell and one HPGe detector (particle-γ) or when at least two HPGe detectors ($\gamma - \gamma$) were in coincidence.

The particle-γ coincidence data were sorted in three matrices depending on the position of the HPGe detectors. A projection of the particle-γ matrix obtained with γ-ray detection at 142° is shown in Fig. 1(a). The γ rays in coincidence with ^{8}Be (or 2α) are shown in Fig. 1(b). This spectrum is dominated by the 727-keV, the 405-keV and the 223-keV lines that are the γ-ray transitions depopulating the first three yrast states of ^{212}Po [18]. Besides some contaminants from ^{211}Po, all other γ rays in the spectrum in Fig. 1(b) originate from the decay of excited states of ^{212}Po [18, 20–23]. Most of these states have been populated in another α-transfer reaction, namely ^{208}Pb(^{18}O,^{14}C) [18]. In addition, we have populated two non-yrast 2^+ states at excitation energies of 1512 keV and of 1679 keV, respectively [20]. These two states decay predominantly to the 2^+_1 state via the 785-keV and the 952-keV transitions, respectively [24]. Both transitions have a well pronounced $M1$ character with multipole mixing ratios of +0.09(3) and +0.65(50) [20], respectively. That makes these two 2^+ states potential candidates for the one-phonon MSS of ^{212}Po. The only missing piece of experimental information that is needed to verify this hypothesis is the large $M1$ transition strengths corresponding to short lifetimes of these levels.

Both the 785-keV and 952-keV lines indeed show well-pronounced Doppler shapes which allows for the lifetimes determination of the 2^+_2 and 2^+_3 states of ^{212}Po by means of the Doppler Shift Attenuation Method (DSAM) (cf. Ref. [25] and references therein). We have performed two parallel analyses of the line shapes; in the first analysis, labelled here Analysis I, we used a Monte Carlo (MC) simulation by means of a modified [26, 27] version of the program DESASTOP [28] in order to describe the slowing down of the recoiling nuclei. The electronic stopping powers used were obtained from the Northcliffe and Schilling tables [29] with corrections for the atomic structure of the medium, as discussed in Ref. [30]. An empirical reduction of $f_n = 0.7$ was applied [31] to downscale the nuclear stopping power predicted by the theory of Lindhard, Scharff, and Schiøtt [32]. The second analysis, labelled Analysis II, uses an integrated software named APCAD (Analysis Program for Continuous Angle DSAM) [33]. In APCAD, the slowing down process is simulated by GEANT4 [34], with the electronic stopping process modelled in the same way as in Analysis I. On the other hand, APCAD adopts a simpler approach to modelling the nuclear stopping process, compared with the completely discrete approach used in Analysis I. In Analysis II the angular straggling due to nuclear collisions is modelled discretely by means of MC simulation while the corresponding energy loss is considered to emerge as a result from a continuous process as the nuclear stopping powers were taken from SRIM2013 [35] and reduced by 30%. Both analyses account for the response of the HPGe detectors, for the experimental geometry, and for the restrictions on the reaction kinematics imposed by the solar cell array. The feeding histories of the levels of interest were determined from the $\gamma-\gamma$ coincidence data. Slow feeding was introduced and fitted in the analyses only if the analysed transitions were observed in coincidence with transitions from higher-lying states. Otherwise, only very fast feeding which can be associated with direct population of the levels of interest, was considered. Under the above assumptions both analyses produced similar results. For example, the lifetime of the 6^- state at 2016 keV is known to be 0.49(16) ps [18]. The lifetime of this level derived in our analyses from the line shape of the 661.3-keV transition, with a feeding history similar to the one used in Ref. [18] (58% fast feeding and 42% slow feeding), is 0.50(4) ps in Analysis I and 0.46(4) ps in Analysis II. The lifetimes of the 2^+_2 state at 1512 keV and 2^+_3 state at 1679 keV were extracted from the line shapes of the 785-keV and the 952-keV transitions, respectively. Both of these transitions are in coincidence with the 727-keV ($2^+_1 \rightarrow 0^+_1$) transition, only. Therefore only fast feeding ($\tau_{feeding} \leq 10$ fs) was introduced in the fits of their lineshapes. In Fig. 2, examples of these fits are presented. The final lifetimes together with

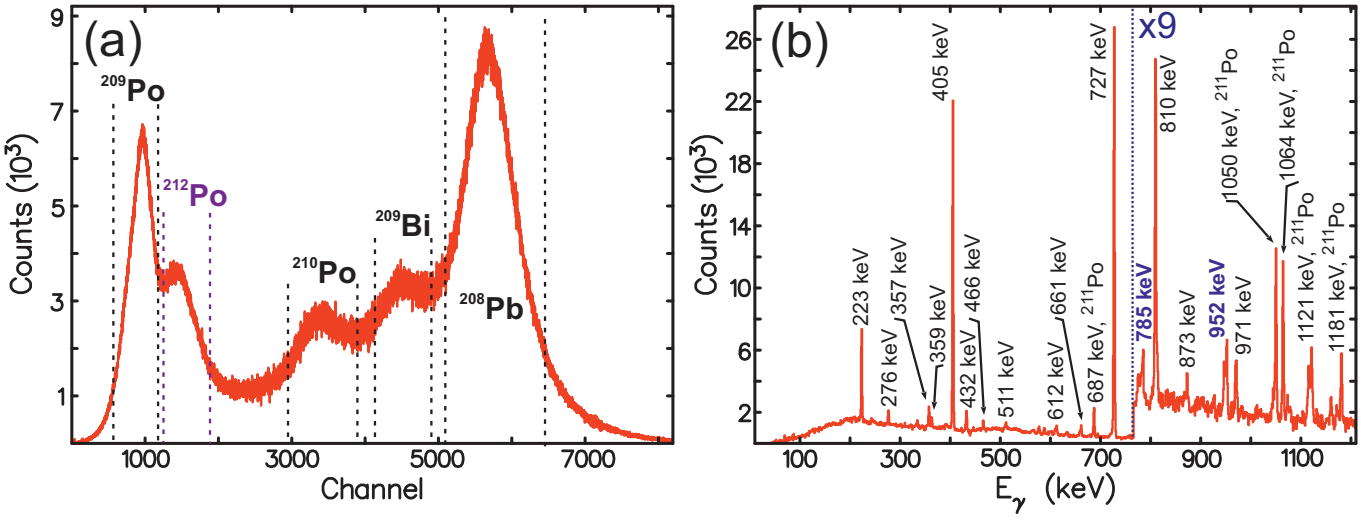

FIG. 1. (Color online) (a) The projection of the particle-γ(@142°) matrix. The vertical dashed lines represent parts of the particle spectrum found to be in coincidence with the γ rays from the indicated nuclei. (b) The γ-ray spectrum in coincidence with the group of particles indicated as "^{212}Po" in panel (a). The transitions connecting the 2_2^+ and the 2_3^+ states to the 2_1^+ state are given in (blue) bold.

the available spectroscopic information and the resulting transition strengths are summarized in Table I. The quoted uncertainties of the results for the lifetimes from Analysis I and II include statistical uncertainties from the line-shape fits and 10% uncertainty in the nuclear and electronic stopping powers. The adopted values are taken as average between the results from both analyses. Finally, we would like to point out that the derived lifetimes in our experiment are in very good agreement with preliminary results from another α-transfer experiment devoted to ^{212}Po which has been conducted at the University of Jyväskylä by A. Astier *et al.* [36].

As seen from Table I, the 2_2^+ state of ^{212}Po at 1512-keV excitation energy decays with a sizeable $M1$ transition to the 2_1^+ state. This allows us to conclude that the 2_2^+ state of ^{212}Po has isovector nature and as such it can be considered, at least, as a fragment of the one-phonon MSS. On the other hand, all observed $B(E2)$ strengths in the decays of the 2_2^+ and the 2_3^+ states are extremely low (cf. Table I) and the yrast states of ^{212}Po form a seniority-like excitation pattern (cf. Fig. 3). These observations indicate the lack of quadrupole collectivity in these low-energy states and question the applicability of the phonon picture for this open-shell nucleus. This situation offers an opportunity to study to what extent the observed sizeable $M1$ strengths can arise from the valence shell configuration, only. The nucleus ^{212}Po has two neutrons and two protons outside the ^{208}Pb core. The simplest possible description of the low-lying states of this nucleus can be pursued in the framework of an empirical single-j shell model approximation. In this approach, the two neutrons are in the $2g_{9/2}$ shell and the protons are in the $1h_{9/2}$ shell. The interactions between the valence particles as well as the effective electromagnetic operators are derived from the experimental data for the neighbouring nuclei as follows. In the single-j shell approximation, ^{210}Pb corresponds to two neutrons in the $2g_{9/2}$ orbital while ^{210}Po corresponds to two protons in the $1h_{9/2}$ orbital with respect to the ^{208}Pb core. Both these nuclei display seniority spectra [37] that are consistent with the single-shell hypothesis. The energy spectrum of ^{210}Bi determines the interaction between a neutron in the $2g_{9/2}$ orbital and a proton in the $1h_{9/2}$ orbital, and the entire multiplet from 0^- to 9^- is known [37]. In the single-j shell approximation, the basis states of ^{212}Po can be written as $|(2g_{9/2})^2 J_\nu, (h_{9/2})^2 J_\pi; J\rangle \equiv |J_\nu J_\pi J\rangle$. The proton-proton and neutron-neutron interactions are diagonal in this basis which is mixed by the proton-neutron interaction,

$$\langle J_\nu J_\pi J|\hat{H}|J'_\nu J'_\pi J\rangle = (V_{\nu\nu}^{J_\nu} + V_{\pi\pi}^{J_\pi})\delta_{J_\nu J'_\nu}\delta_{J_\pi J'_\pi} + \\ + 4\sqrt{(2J_\nu+1)(2J_\pi+1)(2J'_\nu+1)(2J'_\pi+1)} \times \sum_R (2R+1) \begin{bmatrix} j_\nu & j_\pi & J_\pi & J_\nu \\ R & j_\pi & J & j_\nu \\ j_\nu & j_\pi & J'_\pi & J'_\nu \end{bmatrix} V_{\pi\nu}^R,$$

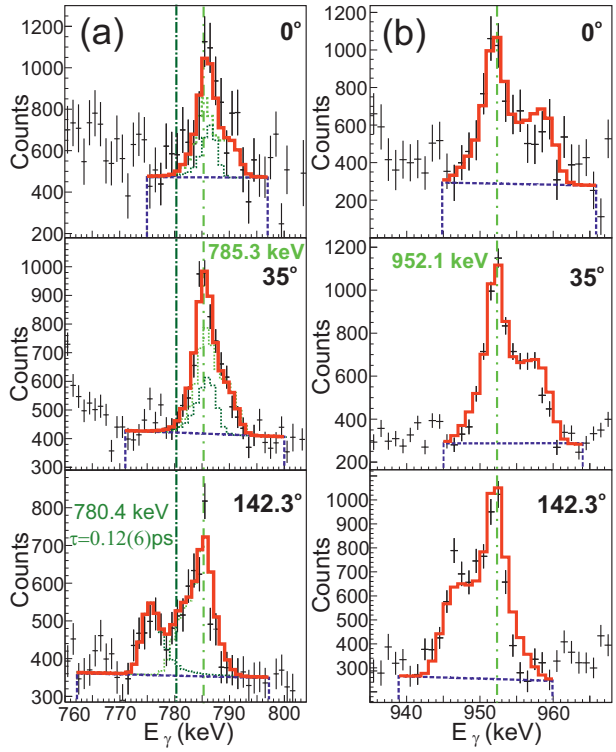

FIG. 2. (Color online) An example of line-shape fits of the 785.3-keV ($2_2^+ \rightarrow 2_1^+$)(a) and the 952.1-keV ($2_3^+ \rightarrow 2_1^+$) (b) transitions obtained with the program APCAD. The dashed (blue) lines show the background and the fit regions. The solid (red) line represents the total fit. The 785-keV line is fitted simultaneously with the 780.4-keV line which originates from the decay of the $7^{(+)}$ state of ^{212}Po at the excitation energy of 3155 keV ($\tau = 0.12(6)$ps) [18]. The dotted lines (green and grass green) represent the individual contributions of 785-keV and 780-keV lines to the total fit. The vertical dash-dotted lines show the position of the unshifted peaks.

TABLE I. Properties of the 2_2^+ and the 2_3^+ states of ^{212}Po and γ-ray transitions originating from their decays. Given are the excitation energies (E_{level}), the spin and parity quantum numbers of the levels (J^π) and of the final levels (J^π_{final}), the energies (E_γ), the relative intensities (I_γ), the total electron conversion coefficients (α), and the multipole mixing ratios (δ) of the γ-rays transitions, the lifetimes of the states, and the absolute transition strengths.

E_{level} (keV)	J^π	J^π_{final}	E_γ (keV)	I_γ [a] %	α [b]	δ [c]	τ (ps) Analysis I	τ (ps) Analysis II	τ (ps) Adopted	Transition strength $J^\pi \rightarrow J^\pi_{final}$ [d]
1512	2_2^+	0_1^+	1512.7	26(3)			0.73(7)	0.69(6)	0.71(9)	$B(E2) = 29(4)$
		2_1^+	785.4	100(1)	0.0408(2)	0.09(3)				$B(M1) = 0.126(16)$
										$B(E2) = 24(16)$
1679	2_3^+	0_1^+	1679.7	35(8)			0.82(4)	0.74(7)	0.78(8)	$B(E2) = 20(5)$
		2_1^+	952.1	100(19)	0.020(5)	0.65(50)				$B(M1) = 0.042(20)$
										$B(E2) = 290(273)$

[a] From Ref. [24].
[b] Total electron conversion coefficients. From Ref. [24].
[c] From Ref. [21].
[d] $B(E2)$ values are given in e^2fm^4 (1 W.u.= 75.09 e^2fm^4), and the $B(M1)$ values are given in μ_N^2. In the calculations for the transitions strengths vanishing α-decay branches were assumed.

where $V^{J_\nu}_{\nu\nu}$, $V^{J_\pi}_{\pi\pi}$, and $V^{R}_{\pi\nu}$ are the neutron-neutron, proton-proton and proton-neutron interaction matrix elements, respectively, and the symbol in square brackets is a 12j coefficient of the second kind [38]. In the single-j shell approximation the $M1$ operator is entirely determined from the magnetic moments of the ground states of ^{209}Pb and ^{209}Bi, $\mu(9/2^+_1) = -1.4735(16)\mu_N$ and $\mu(9/2^-_1) = +4.1103(5)\mu_N$ [39]. This yields a neutron g factor of $g_\nu = -0.33$ and a proton g factor of $g_\pi = +0.91$. In ^{210}Pb and ^{210}Po there are several known $B(E2)$ values for transitions between the lowest-lying yrast states. Amongst them, the lowest $B(E2)$'s are observed for the $8^+_1 \rightarrow 6^+_1$ transitions, $53(23)\mathrm{e}^2\mathrm{fm}^4$ in ^{210}Pb and $84(3)\mathrm{e}^2\mathrm{fm}^4$ in ^{210}Po. Consequently, it can be assumed that the 8^+_1 and 6^+_1 states of these nuclei have pure two-nucleon configurations. Therefore, the effective proton and neutron charges in the $E2$ transition operator were determined from the measured $B(E2; 8^+_1 \rightarrow 6^+_1)$ values for ^{210}Pb and ^{210}Po. This approach yields the effective charges $e_\nu = 1.04$ and $e_\pi = 1.52$.

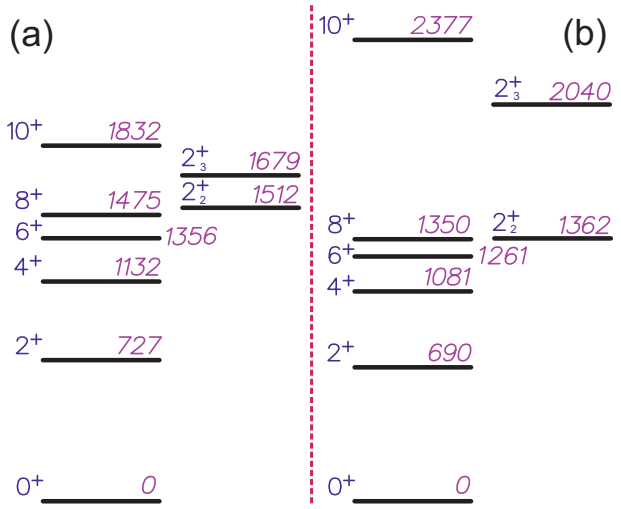

FIG. 3. (Color online) Comparison of experimental low-lying excited states of ^{212}Po (a) with the calculated ones (b) (for details see the text). The energies of the levels are given in keV.

Calculated level energies are compared with experimental ones in Fig. 3. The energies for most of the states, except for 10^+_1 and 2^+_3, are well reproduced. Apparently, the 10^+_1 and 2^+_3 states have more complicated structures outside the considered model space. For the rest of the states, the calculated spectrum closely follows the experimentally-observed energy pattern with some energy compression. The latter leads to deviations between the observed and the calculated level energies in the range between 37 keV (for the 2^+_1) to 150 keV (for the 2^+_2). The 2^+_2 state is correctly reproduced to appear slightly higher than the 8^+_1 state. We stress that this description is not a fit to the data on ^{212}Po but rather, an extrapolation of the data on neighbouring nuclides to ^{212}Po based on the hypothesis of a structure dominated by the $1h_{9/2}$ and $2g_{9/2}$ orbitals.

TABLE II. Comparison between the experimental and the calculated (for details see the text) transition strengths for decays of the low-lying states in ^{212}Po.

Transition	$B(M1; J_i \rightarrow J_f)(\mu^2_\mathrm{N})$		$B(E2; J_i \rightarrow J_f)(\mathrm{e}^2\mathrm{fm}^4)$	
$J_i \rightarrow J_f$	Experiment	Theory	Experiment	Theory
$2^+_1 \rightarrow 0^+_1$	–	–	–	463
$4^+_1 \rightarrow 2^+_1$	–	–	–	533
$6^+_1 \rightarrow 4^+_1$	–	–	293 (83)[a]	300
			1051(300)[b]	
$8^+_1 \rightarrow 6^+_1$	–	–	173 (68)[a]	103
			353(9)[b]	
$10^+_1 \rightarrow 8^+_1$	–	–	165 (45)[a]	75
$2^+_2 \rightarrow 0^+_1$	–	–	29 (4)[c]	59
$2^+_2 \rightarrow 2^+_1$	0.126(16)[c]	0.46	24 (16)[c]	17
$2^+_3 \rightarrow 0^+_1$	–	–	20 (5)[c]	7
$2^+_3 \rightarrow 2^+_1$	0.042(20)[c]	0.0003	290 (273)[c]	186

[a] From data given in Ref. [24].
[b] From data given in Ref. [18].
[c] From the present work (cf. Tab. I).

The comparison between the known and the observed transition strengths (see Tab. II) is more ambiguous; there are severe discrepancies in the literature values for the α-decay branching ratios of the 6^+_1 and the 8^+_1 states (see Refs. [24] and [18]). Therefore, it is difficult to judge to what extent the model reproduces the experimental $B(E2)$ transition strengths for the yrast states. However, an agreement between the results from calculations based on a simple seniority scheme and the experimental $B(E2)$ values cannot be expected as the 6^+_1 and the 8^+_1 states of ^{212}Po may include an α-cluster structure, as discussed in Ref. [18]. At the same time, the agreement between the experimental and the calculated transitions strengths for the non-yrast states is, at least qualitatively, good even for the 2^+_3 state (see the bottom lines in Tab. II). More importantly, the model predicts that the 2^+_2 state decays with a very strong $M1$ transition to the 2^+_1 state - in qualitative agreement with the observed sizeable value of $0.126(16)\mu^2_\mathrm{N}$. Thus, the model accounts qualitatively well for the main isovector features of the low-lying states of ^{212}Po which allows to trace the origin of the $M1$ strength to the structure of the 2^+_1 and 2^+_2 states. The wave functions of these states can be presented as follow:

$$|2^+_1\rangle = 0.448|J_\nu = 0, J_\pi = 2, J = 2\rangle + 0.819|J_\nu = 2, J_\pi = 0, J = 2\rangle + \cdots$$
$$|2^+_2\rangle = 0.813|J_\nu = 0, J_\pi = 2, J = 2\rangle - 0.517|J_\nu = 2, J_\pi = 0, J = 2\rangle + \cdots$$

The two components in the wave functions, which can be thought of as proton and neutron S and D pairs, exhaust about 87% and 93% of the total wave functions of the 2_1^+ and the 2_2^+ states, respectively. The main difference between these wave functions is the opposite sign of the dominant proton and neutron components. This reveals the isovector nature of the wave function of the 2_2^+ state which leads to the enhanced $B(M1; 2_2^+ \rightarrow 2_1^+)$ value. Apparently, even extremely simple shell models, like the one used here, tend to generate low-lying isovector states based on two particle - two hole excitations. The isovector nature of these states remains preserved in reality, where the extremely simplified wave functions presented above mix with more complex configurations. In this respect, the isovector character of the collective states, such as MSSs, can be regarded as a feature which already appears solely from the single-particle valence shell configuration.

In summary, by using data from an α-transfer reaction leading to ^{212}Po, we have determined the lifetimes of two non-yrast 2^+ states. These states were considered as candidates for the one-phonon MSS of this nucleus. The resulting absolute transitions strengths reveal the predominant isovector nature of the 2_2^+ state. This represents the first identification of a low-lying isovector state in a nucleus from the mass region around the double-magic nucleus ^{208}Pb. The experimental data also reveals a weakened quadrupole collectivity in these non-yrast states which questions the applicability of the phonon picture in ^{212}Po. Instead, the data for the off-yrast states is qualitatively well described in the framework of a single-j empirical shell model which represents an extreme single-particle approximation. All these findings indicate that the isovector nature of low-lying states is a property of the leading valence single-particle configuration.

Acknowledgements: G.R. acknowledges the support from the Alexander von Humboldt foundation. This work was supported by the partnership agreement between the University of Cologne and University of Sofia, by the German-Bulgarian exchange program under grants DAAD No. PPP57082997 and BgNSF No. DNTS/01/05/2014, by the DFG under grant Pi393/2-3, and by the BMBF under grants 05P12RDCIB, 05P12RDFN8 and 05P15RDCIA.

[1] N. Lo Iudice and F. Palumbo, Phys. Rev. Lett. **41**, 1532 (1978).
[2] F. Iachello, Phys. Rev. Lett. **53**, 1427 (1984).
[3] F. Iachello and A. Arima, *The interacting boson model* (Cambridge University Press, Cambridge, 1987).
[4] N. Pietralla, P. von Brentano, A.F. Lisetskiy, Prog. Part. Nucl. Phys. **60**, 225 (2008) and the references therein.
[5] K. Heyde, P. von Neumann-Cosel, A. Richter, Rev. Mod. Phys. **82**, 2366 (2010).
[6] G. Rainovski *et al.*, Phys. Rev. Lett. **96**, 122501 (2006).
[7] T. Ahn *et al.*, Phys. Lett. **B679**, 19 (2009).
[8] L. Coquard *et al.*, Phys. Rev. C **82**, 024317 (2010).
[9] K.A. Gladnishki *et al.*, Phys. Rev. C **82**, 037302 (2010).
[10] M. Danchev *et al.*, Phys. Rev. C **84**, 061306(R) (2011).
[11] T. Ahn *et al.*, Phys. Rev. C **86**, 014303 (2012).
[12] K. Heyde and J. Sau, Phys. Rev. C **33**, 1050 (1986).
[13] C. Walz *et al.*, Phys. Rev. Lett. **106**, 062501 (2011).
[14] J.D. Holt, N. Pietralla, J.W. Holt, T.T.S. Kuo, G. Rainovski, Phys. Rev. C **76**, 034325 (2007).
[15] V. Werner *et al.*, Phys. Lett. **B550**, 140(2002); V. Werner *et al.*, Phys. Rev. C **78**, 031301(R) (2008).
[16] D. Bianco, N. Lo Iudice, F. Andreozzi, A. Porrino, F. Knapp, Phys. Rev. C 88, 024310 (2011).
[17] D.C. Radford *et al.*, Phys. Rev. Lett. **88**, 222501 (2002).
[18] A. Astier, P. Petkov, M.-G. Porquet, D.S. Delion, and P. Schuck, Phys. Rev. Lett. **104**, 042701 (2010); A. Astier, P. Petkov, M.-G. Porquet, D.S. Delion, and P. Schuck, Eur. Phys. J. A **46**, 165 (2010).
[19] A. Dewald, O. Möller, P. Petkov, Prog. Part. Nucl. Phys. **67**, 786 (2012).
[20] B. Bengtson *et al.*, Nucl. Phys. A **378**, 1 (1982).
[21] A.R. Poletti *et al.*, Nucl. Phys. A **473**, 595 (1987).
[22] Zs. Podolýak *et al.*, Nucl. Instrum. Methods Phys. Res. A **511**, 354 (2003).
[23] A.B. Garnsworthy *et al.*, J. Phys. G **31**, S1851 (2005).
[24] E. Browne, Nucl. Data Sheets **104**, 427 (2005).
[25] T.K. Alexander and J.S. Forster, Adv. Nucl. Phys. **10**, 197 (1978).
[26] P. Petkov *et al.*, Nucl. Phys. A **640**, 293 (1998).
[27] P. Petkov *et al.*, Nucl. Instrum. Methods Phys. Res. A **431**, 208 (1999).
[28] G. Winter, ZfK. Rossendorf Report ZfK-497, 1983; G. Winter, Nucl. Instrum. Methods **214**, 537 (1983).
[29] L.C. Northcliffe and R.F. Schilling, Nucl. Data Sect. **7**, 233 (1970).
[30] J.F. Ziegler and J.P. Biersack, in *Treatise on Heavy Ion Science*, edited by D.A. Bromley (Plenum Press, New York, 1985), Vol. 6, p. 95.
[31] J. Keinonen, AIP Conf. Proc. **125**, 557 (1985).
[32] J. Lindhard, M. Scharff, and H.E. Schiøtt, Kgl. Dan. Vid. Selsk. Mat. Fys. Medd. **33**, 14 (1963).
[33] C. Stahl, PhD thesis, TU Darmstadt (2015).
[34] S. Agostinelli *et al.*, Nucl. Instrum. Methods Phys. Res. A **506**, 250 (2003).
[35] J.F. Ziegler, M.D. Ziegler, J.P. Biersack, Nucl. Instr Meth., B **268**, 1823 (2010).
[36] A. Astier *et al.*, to be published.
[37] M. Shamsuzzoha Basunia, Nucl. Data Sheets **121**, 561 (2014).
[38] A.P. Yutsis, I.B. Levinson and V.V. Vanagas, The Theory of Angular Momentum (Israel Program for Scientific Translations, Jerusalem, 1962).
[39] J. Chen and F.G. Kondev, Nucl. Data Sheets **126**, 373 (2015).